# Vibration serviceability of footbridges: Evaluation of the current codes of practice

K. Van Nimmen[a,b], G. Lombaert[a], G. De Roeck[a], P. Van den Broeck[a,b]

[a] *Department of Civil Engineering, KU Leuven, Kasteelpark Arenberg 40, B-3001 Leuven, Belgium*

[b] *Department of Engineering Technology, KAHO Sint-Lieven, Gebr. De Smetstraat 1, B-9000 Ghent, Belgium*

**Abstract**

Contemporary footbridges are often designed as slender structures and tend to be susceptible to human induced vibrations. Codes of practice have been developed enabling the designer to evaluate the vibration serviceability of the structure based on simplified load models to simulate crowd induced loading.

This paper evaluates the methodology of the recent European guideline HiVoSS and the French guideline Sétra, which are widely applied in practice. For a selection of eight slender footbridges, the assessment is performed in design stage, based on the available finite element model, and at completion, based on the in situ identified modal characteristics. Comparison of the initially predicted and the in situ identified modal characteristics shows that uncertainty with respect to the predicted dynamic properties of the structure is inevitable. The methodologies are, however, sensitive to small variations in modal parameters, such as the natural frequencies. As a result, the guidelines in their current form could be exploited by designers to tune the dynamic characteristics of the structure in order to pass the vibration serviceability check. The present contribution recommends a modified load model that leads to a more robust vibration serviceability assessment.

*Keywords:* footbridge, vibration serviceability, human induced vibrations, guidelines

*Corresponding author. Tel.: +32 (0)9 265 86 12.
*Email address:* katrien.vannimmen@bwk.kuleuven.be (K. Van Nimmen)

*Preprint submitted to Engineering Structures*
*Published version:* http://dx.doi.org/10.1016/j.engstruct.2013.11.006

## 1. Introduction

Slender footbridges are often highly susceptible to human induced vibrations, due to their low stiffness, damping and modal mass [1]. During the last decade, numerous problems with vibration serviceability have been reported, none of which as widely discussed as London's Millennium [2, 3] and Paris' Solférino footbridge [4]. In order to ensure user comfort and safety, many footbridges today are equipped with tuned mass dampers, e.g. the Pedro e Inês footbridge [5, 6], the Changi Mezzanine Bridge [7, 8], the Van Beethoven footbridge [9], the footbridge of VW Autostadt [10], the Kurilpa footbridge [11] and the Northshore footbridge [12].

Predicting the dynamic response of these civil engineering structures under crowd induced loading has therefore become an important aspect of the structural design [13]. Because the walking behaviour is unique for each individual and is influenced by interaction with the structure and synchronisation with other persons present on the structure [14, 15, 16], it is not straightforward to formulate a general model for crowd induced loading [17]. A clear need for practical design procedures exists given the large number of footbridges under construction and in design[1]. Multiple simplified design methodologies have been developed but their evaluation and validation have been given little attention so far. In order to evaluate and further develop these guidelines, applications on real case studies are needed.

The objective of this paper is to review and evaluate the methodology of two current codes of practice, the French Sétra guideline [18] and the European guideline HiVoSS [19, 20], both widely applied in engineering practice. In the evaluation procedures, it is assumed that the dynamical characteristics of the structure, e.g. the natural frequencies and mode shapes, are known. Furthermore, a simplified force model is proposed for the loads due to various densities of the pedestrian traffic on the bridge.

The methodology of the design guides is evaluated for application in design stage, using a finite element model based on structural drawings, and at completion when the footbridge is built and the dynamic characteristics of the structure can be identified in situ. In total, eight lively footbridges are considered in this study. For each case, a finite element model is developed, the modal characteristics are identified and the vibration serviceability is assessed.

The outline of this paper is as follows. First, the methodology of the current codes of practice is discussed. Second, the different case studies are

presented, including a description of the finite element model and the modal parameters as identified from the operational modal analysis. In the final section, the vibration serviceability assessment is performed according to the guidelines in design stage and at completion enabling the evaluation of the design procedures.

## 2. Current codes of practice

This section gives a brief summary of the footbridge vibration serviceability design procedures as described by the French Sétra guideline [18] and the European HiVoSS guideline [19, 20]. The Sétra guideline was developed within the framework of the Sétra/AFGC working group on "Dynamic behaviour of footbridges". The HiVoSS guideline is based on the results obtained within the research project RFS-CR-03019 "Advanced Load Models for Synchronous Pedestrian Excitation and Optimised Design Guidelines for Steel Footbridges (SYNPEX)" [20]. The methodology is discussed in four parts, (1) modelling of the human induced loads, (2) characterisation of the dynamic behaviour of the footbridge, (3) the calculation, and (4) evaluation of the maximum expected vibration levels.

### *2.1. Modelling the human induced loads*

Walking loads have been studied thoroughly in the past and different time-dependent load models have been developed. Conventionally, the walking force is described as a sum of Fourier harmonic components [17]:

$$F(t) = G + \sum_{i=1}^{n} G\alpha_i sin(2\pi f_s - \theta_i) \tag{1}$$

where $G$ [N] is the static weight of the pedestrian, $i$ the order number of the harmonic, $n$ the total number of contributing harmonics, $\alpha_i$ the Fourier coefficient of the $i$-th harmonic normalised to the weight of the pedestrian (generally known as the dynamic loading factor), $f_s$ [Hz] the step frequency and $\theta_i$ [rad] the phase shift of the $i$-th harmonic. In the case where the pedestrian is moving at a constant speed $v$ [m/s] along the centerline of the bridge deck, the force of the pedestrian can be represented as the product of the time component F(t) and a component describing its time-dependent position $\delta(x - vt)$:

$$P(x, t) = F(t)\delta(x - vt) \tag{2}$$

where $\delta$ is the Dirac delta function and $x$ the position of the pedestrian along the bridge centerline.

In practice, footbridges are subjected to the simultaneous actions of groups of pedestrians or crowds [18]. The corresponding load therefore has to account for inter-subject variability as well as intra-subject variability [21]. First, each pedestrian has its own characteristics, e.g. weight, step frequency and walking speed (inter-subject variability). Second, some parameters such as step length and walking speed, may vary along the path (intra-subject variability) [17, 22]. Furthermore, pedestrians will each arrive at a different time and may also synchronise their motion with other pedestrians or the bridge itself [23, 24].

*Equivalent load*

In both Sétra and HiVoSS, the random load due to a stream of $N$ random pedestrians [#persons/s], corresponding to a specific pedestrian density $d$ [persons/m$^2$], is simplified to an equivalent deterministic load which is uniformly distributed on the bridge deck. This simplified load model consists of an equivalent number ($N_{eq}$) of perfectly synchronised pedestrians. This number is derived from numerical simulations and is defined such that the same acceleration level is generated as the 95 percentile-value of the peak accelerations of 500 simulated streams of $N$ random pedestrians.

These underlying numerical simulations make a distinction between *sparse* and *dense* crowd conditions. For low pedestrian densities (d $< 1$ pm$^{-2}$), free movement of the pedestrians is assumed. This assumption results into random arrival times and normally distributed step frequencies centered around a natural frequency of the footbridge. In the case of *dense* crowds (d $\geq 1$ pm$^{-2}$), normal walking behaviour gets obstructed causing the forward movement of the stream to slow down, which is accompanied by an increase of the level of synchronisation. To simulate these *dense* crowd conditions, the random arrival times are retained but all pedestrians are given the same step frequency. This higher level of synchronisation will result in a larger equivalent number of pedestrians. Beyond the upper limit value of 1.5, walking of pedestrians is considered to be impossible, significantly reducing the dynamic effects [19].

The guidelines define the equivalent number of pedestrians $N_{eq}$ as:

$$\begin{aligned} N_{eq} &= 10.8\sqrt{\xi_j N} \text{ for } d < 1 \text{ p/m}^2 \\ N_{eq} &= 1.85\sqrt{N} \quad \text{for } d \geq 1 \text{ p/m}^2 \end{aligned} \tag{3}$$

where $d$ denotes the pedestrian density and $\xi_j$ is the modal damping ratio. The corresponding amplitude $q_{eq,e}$ of the equivalent load [Nm$^{-2}$], in direction $e$ (vertical, lateral or longitudinal) is defined as:

$$q_{eq,e} = \frac{N_{eq}}{S} \alpha_{eh} G \psi_{eh}(f_j) \tag{4}$$

where $f_j$ is the natural frequency of mode $j$ under consideration, $S$ is the bridge deck surface area, $\alpha_{eh}$ is the dynamic load factor of the $h$-th harmonic of the load in direction $e$ generated by a single pedestrian with body weight $G$ [N] (table 2). The factor $\psi_{eh}(f_j)$ (with $0 \leq \psi_{eh}(f_j) \leq 1$ [-]) is the reduction coefficient that accounts for the probability that the step frequency (or its second harmonic) equals the natural frequency of mode $j$ under consideration, and thus the probability that footbridge resonance will occur. This probability of resonance has been determined based on a statistical distribution of possible step frequencies, with a mean pacing rate typically around 2 Hz, and its second harmonic. When the probability of resonance is evaluated with respect to the lateral induced forces, the frequency bounds of the ranges that represent this probability are divided by two which is owed to the particular nature of walking: left and right foot are equivalent in vertical and longitudinal action but opposed in horizontal action [18], which is reducing the excitation frequency by a factor of two (figure 1b). Due to this reduction factor, only modes with a natural frequency less then 5 Hz have to be taken into account in the vibration serviceability assessment.

Figure 1 illustrates the different ranges where resonance may occur. The Sétra guideline refers to 'ranges of risk' to describe this probability of resonance: Range 4 - negligible risk (no calculation required - $\psi_{eh}(f_j) = 0$), Range 3 - low risk of resonance with the 2nd harmonic, Range 2 - medium risk and Range 1 - maximum risk of resonance with the 1st harmonic. The HiVoSS guideline specifies 2 critical ranges of natural frequencies for which a calculation is required: Range 1 - possibility of resonance with the 1st harmonic and Range 2 - possibility of resonance with the 2nd harmonic.

*Footbridge classification*

The guidelines classify a footbridge based on the expected pedestrian traffic: footbridges located in an urban environment are treated differently from those located in rural areas. A governing parameter in assessing the vibration serviceability is thus the expected pedestrian density. The Sétra guideline defines 4 classes: low (Class IV) and normal use (Class III), urban

| | Pedestrian density $d$ | | | | | |
|---|---|---|---|---|---|---|
| | 15 [p/deck] | 0.2 [p/m$^2$] | 0.5 [p/m$^2$] | 0.8 [p/m$^2$] | 1.0 [p/m$^2$] | 1.5 [p/m$^2$] |
| Sétra | | | Class III | Class II | Class I | |
| HiVoSS | TC 1 | TC 2 | TC 3 | | TC 4 | TC 5 |

Table 1: Traffic classes and corresponding pedestrian densities

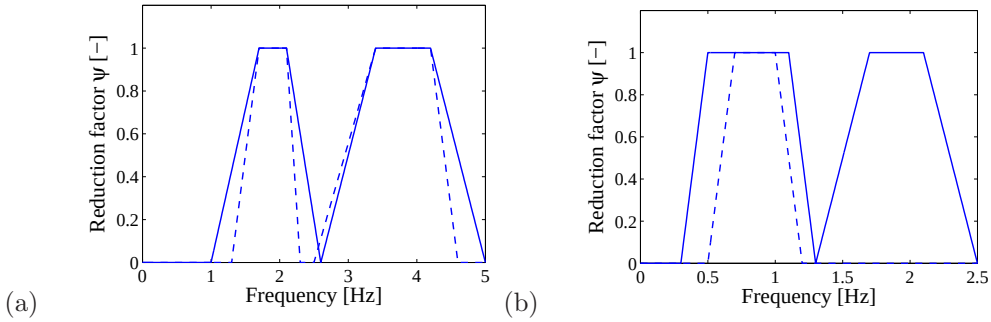


Figure 1: Reduction factor $\psi(f_j)$ according to (-) Sétra and (- -) HiVoSS (a) for vertical and longitudinal loading and (b) for lateral loading.

use (Class II) and urban use with high concentration of pedestrian traffic or with crowds frequently crossing the structure (Class I). The HiVoSS guideline specifies 5 traffic classes varying from very weak (TC 1), weak (TC 2), dense (TC 3), very dense (TC 4) to exceptional dense traffic (TC 5). The corresponding pedestrian densities $d$ [persons/m$^2$] can be found at the top of table 1.

### *2.2. Characterisation of the dynamic behaviour of the footbridge*

The dynamic behaviour of the footbridge near resonance strongly depends on the damping ratio, a parameter which can only be assumed in design stage, based on experience obtained from similar structures. The guidelines suggest minimum and mean values for the damping ratio according to the considered construction type (table 3).

The mass of the pedestrians (70 kg/person) on the bridge deck modifies the natural frequencies and the corresponding modal displacements. The HiVoSS guideline states that the influence of the added modal mass is only to be considered when it exceeds 5% of the modal mass of the unoccupied bridge deck of the considered mode. According to Sétra, the assessment

| direction $e$ | $h=1$ | | $h=2$ | |
|---|---|---|---|---|
| | $\alpha$ [-] | $\alpha G$ [N] | $\alpha$ [-] | $\alpha G$ [N] |
| vertical | 0.40 | 280 | 0.10 | 70 |
| lateral | 0.05 | 35 | 0.01 | 7 |
| longitudinal | 0.20 | 140 | 0.05 | 35 |

Table 2: Dynamic load factor of the $h$-th harmonic of the load generated by a single pedestrian with body weight $G = 700$ N and corresponding force amplitude $\alpha G$.

| Construction type | Damping factor $\xi$ [%] Sétra | | HiVoSS | |
|---|---|---|---|---|
| | min | mean | min | mean |
| Reinforced concrete | 0.8 | 1.3 | 0.8 | 1.3 |
| Prestressed concrete | 0.5 | 1.0 | 0.5 | 1.0 |
| Steel | 0.2 | 0.4 | 0.2 | 0.4 |
| Mixed | 0.3 | 0.6 | 0.3 | 0.6 |
| Timber | 1.5 | 3.0 | 1.0 | 1.5 |
| Stress-ribbon | - | - | 0.7 | 1.0 |

Table 3: Damping factor $\xi$ [%] suggested by the guidelines for different construction types.

should consider the range of natural frequencies for which the upper limit is determined by the empty footbridge and the lower limit is found by adding a uniformly distributed mass corresponding to the highest pedestrian density.

### *2.3. Calculation of the vibration levels*

The maximum acceleration levels $\ddot{u}_{j,e\,\max}$ in direction $e$ are calculated considering resonant conditions for mode $j$ of the structure. The guidelines assume that the response of the structure is dominated by the contribution of the considered mode $j$ which can therefore be calculated as:

$$\ddot{u}_{j,e\,\max} = q_{eq,e} \frac{\sum_i S_i \left|\varphi_{j,p(i)e}\right|}{2\xi_j} \max_{p(i)} \left[\left|\varphi_{j,p(i)e}\right|\right] \tag{5}$$

with $\ddot{u}_{j,e\,\max}$ [m/s$^2$] the maximum acceleration in direction $e$, $q_{eq,e}$ [N/m$^2$] the amplitude of the equivalent load in direction $e$, $S_i$ the discretisation of the bridge deck surface area ($S = \sum S_i$), $p(i)$ the position on the bridge deck according to the discretisation, $\varphi_{j,p(i)e}$ $\left[1/\sqrt{kg}\right]$ the mass normalised modal displacement of mode $j$, i.e. assuming $\Phi^{\mathrm{T}}\mathrm{M}\Phi = \mathrm{I}$, at position $p(i)$ and in

| | **Acceleration** [m/s$^2$] | | | | |
|---|---|---|---|---|---|
| **Vertical** | $< 0.5$ | 0.5 | 1.0 | 2.5 | $> 2.5$ |
| Sétra | max | mean | min | unacc | |
| HiVoSS | max | mean | min | unacc | |

| **Horizontal** | $< 0.15$ | 0.15 | 0.3 | 0.8 | $> 0.8$ |
|---|---|---|---|---|---|
| Sétra | max | mean | min | unacc | |
| HiVoSS | max | mean | min | unacc | |
| | 0.1 | | | | |

Table 4: Comfort levels (maximum, minimum, mean and unacceptable) and corresponding acceleration ranges for vertical and horizontal vibrations

direction $e$, and $\xi_j$ [-] the corresponding damping ratio. The equivalent load at position $p(i)$ on the bridge deck is chosen such that the modal load is maximised, which results in the absolute value of the modal displacements in equation (5).

Note that the predicted maximum acceleration levels only depend on the natural frequency of the considered mode $j$ through the reduction factor $\psi_{eh}(f_j)$ in the equivalent load $q_{eq,e}$ (equation 4).

*2.4. Evaluation of the vibration levels*

The perception of vibrations is subjective and strongly depends on the vibration direction, the duration of exposure as well as the receivers' posture and activities [25]. As a result, it is difficult to determine clear thresholds in relation to the comfort perceived by the pedestrian [26, 27, 28]. Bearing this in mind, the guidelines present four intervals of acceleration levels with corresponding comfort level, ranging from unacceptable vibration levels to maximum comfort. The ranges for vertical and horizontal (lateral and longitudinal) vibrations are presented in table 4.

For every pedestrian density, the predicted maximum acceleration levels $\ddot{u}_{j,e\,\max}$ allow assessing the level of comfort in each vibration direction. In this way, critical modes for which the vibration serviceability may not be fulfilled are identified.

The guidelines also warn against the lock-in phenomenon which can be triggered by lateral acceleration levels exceeding 0.1 to 0.15 m/s$^2$. Below this threshold, pedestrian behaviour can be considered to be random. As soon as the threshold is passed, the rate of synchronisation rises significantly as well as the acceleration level, where it may become uncomfortable for high pedestrian densities [18, 19].

*2.5. Comparison*

The methodologies of the Sétra and HiVoSS guideline are highly similar but sometimes differ in the load cases that have to be considered. This is illustrated by the fact that they present another selection of pedestrian densities and a different estimation of the possibility that resonance may occur, e.g. the HiVoSS guideline does not consider the second harmonic of the lateral load. Figure 1 also illustrates the small differences in the applied reduction factor, which result into a different amplitude of the equivalent load.

The guidelines also present slightly different approaches to account for the modification of the dynamic behaviour of the structure due to the added mass of the pedestrians. According to the Sétra guideline, the natural frequencies of the footbridge are determined for the empty structure and the structure considering an added mass of 70 kg for each pedestrian, distributed over the entire bridge deck surface. These frequencies make up the upper and lower bound respectively of the range of the natural frequency that is used to assess the possibility of resonance for a given mode. In case of the HiVoSS guideline, one has to account for the additional modal mass once the latter exceeds 5% of the modal mass of the unoccupied bridge deck.

## 3. Case studies

A total of 8 footbridges has been studied, all of which were built within the last 10 years. For each case, a finite element (FE) model is developed to simulate the physical behaviour of the structure and to enable the prediction of the response under human induced loading. The main characteristics of these footbridges and the finite element models are listed in table 5. Figure 3 presents the elevation and cross section of the tested structures on a uniform scale.

For all cases, an extensive measurement campaign was carried out to obtain the operational modal characteristics. Output-only system identification is performed based on ambient vibrations, mainly due to wind and nearby highway traffic. The output-only data have been processed using the following OMA algorithm: reference-based data-driven stochastic subspace identification (SSI-data/ref) [29, 30, 31]. The identified modal characteristics for modes with frequencies up to 10 Hz are presented in table 6, together with the predicted natural frequencies of the numerical model (FE model),

| Case study | Characteristics | FE Model |
|---|---|---|
| **Eeklo footbridge**<br>Built: 2002<br>Length: 96m<br>Width: 3m | Steel structure with U-shaped cross section | 1374 beam elements (stiffeners)<br>2640 shell elements (bridge deck)<br>1144 solid elements (concrete pillars)<br>48 spring elements (boundary conditions) |
| **Wetteren footbridge**<br>Built: 2004<br>Length: 107m<br>Width: 3.5m | Steel tied-arch bridge | 44 truss elements (cables)<br>828 shell elements (bridge deck)<br>1338 beam elements (stiffeners and bows) |
| **Ninove footbridge**<br>Built: 2004<br>Length: 58.5m<br>Width: 2.5m | Steel cable-stayed bridge with a 3D truss structure for the bridge deck | 12 truss elements (cables)<br>1631 shell elements (pylon)<br>843 beam elements (stiffeners)<br>24 spring elements (boundary conditions) |
| **Knokke footbridge**<br>Built: 2008<br>Length: 106m<br>Width: 3m | Structural steel *hammock* in which the concrete deck lies | 1760 beam elements (stiffeners)<br>12942 shell elements (steel plates)<br>3456 solid elements (concrete) |
| **Leuven footbridge**<br>Built: 2009<br>Length: 23m<br>Width: 5m | Steel structure | 4680 beam elements (stiffeners)<br>24 spring elements (boundary conditions) |
| **Anderlecht footbridge**<br>Built: 2010<br>Length: 57m<br>Width: 4.8m | Steel arch bridge | 4070 beam elements (stiffeners)<br>12 spring elements (boundary conditions) |
| **Mechelen footbridge**<br>Built: 2011<br>Length: 31m<br>Width: 3m | Steel structure with an L-shaped cross section | 968 beam elements (stiffeners)<br>2904 shell elements (steel plates)<br>12 spring elements (boundary conditions) |
| **Brugge footbridge**<br>Built: 2012<br>Length: 57m<br>Width: 2.5m | Steel structure with a U-shaped cross section | 4572 beam elements (stiffeners)<br>254 shell elements (steel plates)<br>84 spring elements (boundary conditions) |

Table 5: Main characteristics of the case studies and the corresponding FE model.

the corresponding Modal Assurance Criterion (MAC [-]) and the relative frequency deviation ($\varepsilon$ [%]), defined as:

$$MAC_{ij} = \frac{\left|\phi_i^{\mathsf{T}} \tilde{\phi}_j\right|^2}{(\phi_i^{\mathsf{T}} \phi_i)(\tilde{\phi}_j^{\mathsf{T}} \tilde{\phi}_j)} \tag{6}$$

$$\varepsilon_j = \frac{f_j - \tilde{f}_j}{\tilde{f}_j} \tag{7}$$

where the experimental identified parameters are denoted by a tilde.

The comparison presented in table 6 clearly illustrates that predicting the dynamic behaviour of structures is difficult, even with refined FE models based on as-built plans. This is due to the poor prior knowledge that is available regarding certain parameters as the stiffnesses of the supports. Based on the presented cases, a deviation of about 10% in natural frequency with respect to those predicted by the initial finite element model is to be expected, with even larger deviations being well possible. Moreover, the numerical models developed in this study are probably more detailed then those usually considered by design offices. When assessing the vibration serviceability, the designer should account for these uncertainties that are clearly inevitable.

Based on the relatively high MAC values, it can be assumed that the developed finite element models generally succeed in predicting the mode shapes quite accurately.

## 4. Vibration Serviceability Assessment

In this section, the vibration serviceability of the considered footbridges is assessed according to the guidelines. First, an evaluation is performed in design stage based on the available finite element model. Second, the assessment is performed at completion based on in situ identified modal characteristics. For reasons of conciseness, the assessment is presented in detail for two cases, the Eeklo and the Anderlecht footbridge, and is followed by a brief summary of the results for all eight footbridges.

### *4.1. In design stage*

In agreement with the information available in the design process, the assessment is performed based on the predicted natural frequencies and mode

(a)  (b) 

(c)  (d) 

(e)  (f) 

(g)  (h) 

Figure 2: Considered case studies: the (a) Eeklo, (b) Wetteren, (c) Ninove, (d) Knokke, (e) Leuven, (f) Anderlecht, (g) Mechelen, and (h) Brugge footbridge

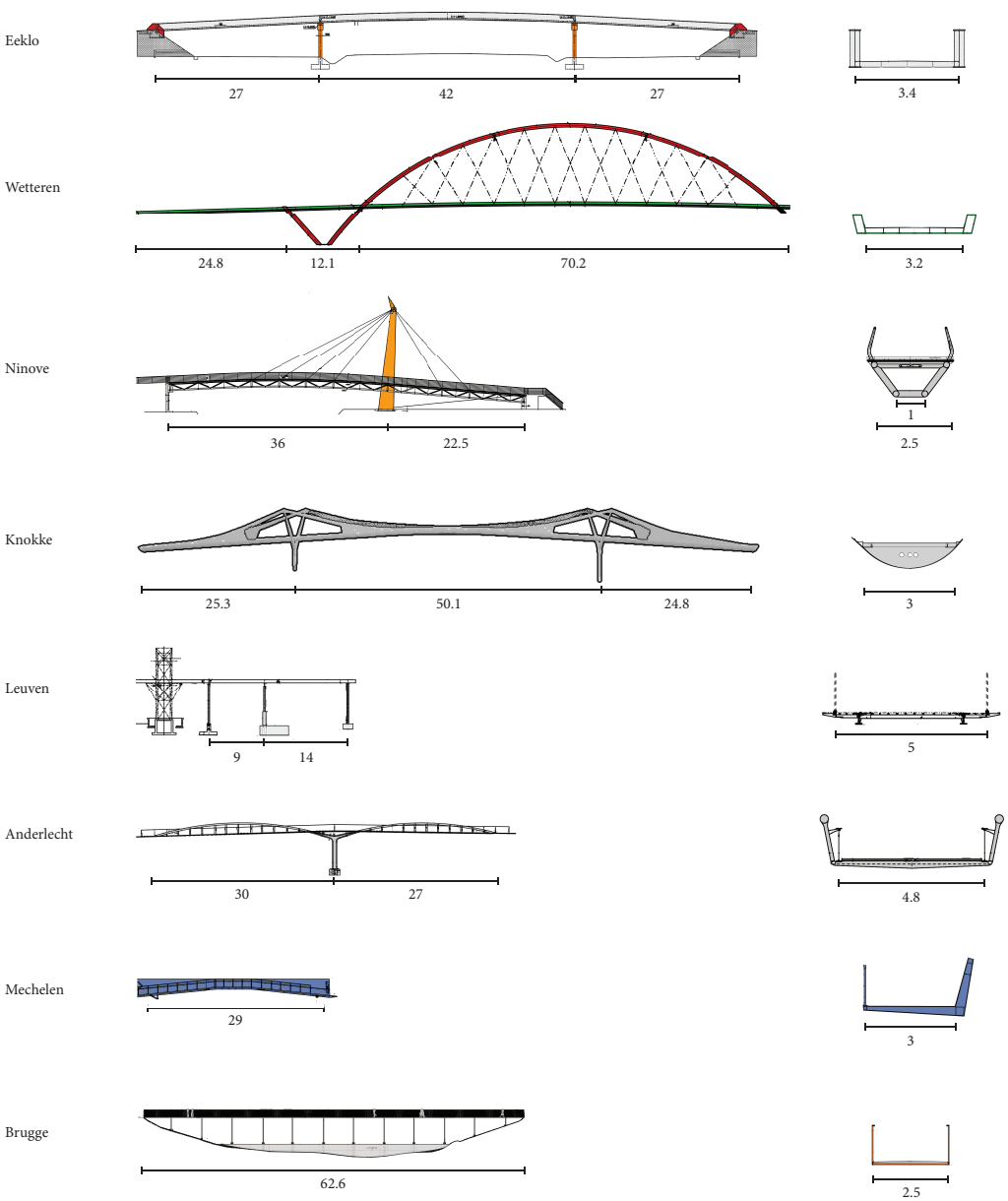


Figure 3: Side views and cross sections of the considered case studies.

**Eeklo footbridge**

| $\tilde{N}$ | $\tilde{f}$ [Hz] | $\tilde{\xi}$ [%] | N | $f$ [Hz] | MAC [−] | $\varepsilon$ [%] |
|---|---|---|---|---|---|---|
| 1 | 1.71 | 1.94 | 1 | 2.03 | 0.94 | **18.8** |
| 2 | 2.99 | 0.19 | 2 | 3.09 | 1.00 | **3.4** |
| 3 | 3.25 | 1.45 | 3 | 4.03 | 0.80 | **24.3** |
| 4 | 3.46 | 2.97 | 4 | 4.79 | 0.77 | **38.7** |
| 5 | 5.77 | 2.97 | 5 | 5.81 | 0.98 | **0.7** |
| 6 | 5.82 | 0.16 | 6 | 5.97 | 0.92 | **2.5** |
| 7 | 6.04 | 2.08 | - | - | - | **-** |
| 8 | 6.47 | 0.60 | 7 | 6.68 | 1.00 | **3.2** |
| 9 | 6.98 | 3.38 | - | - | - | **-** |
| 10 | 7.44 | 4.77 | - | - | - | **-** |

**Anderlecht footbridge**

| $\tilde{N}$ | $\tilde{f}$ [Hz] | $\tilde{\xi}$ [%] | N | $f$ [Hz] | MAC [−] | $\varepsilon$ [%] |
|---|---|---|---|---|---|---|
| 1 | 2.85 | 0.45 | 27 | 3.04 | 0.99 | **6.7** |
| 2 | 3.24 | 0.31 | 28 | 3.11 | 0.70 | **-4.0** |
| 3 | 3.98 | 0.29 | 29 | 3.79 | 0.99 | **-4.8** |
| 4 | 4.22 | 0.39 | 36 | 4.50 | 0.95 | **6.6** |
| 5 | 5.37 | 0.29 | 40 | 5.24 | 0.92 | **-2.4** |
| 6 | 6.21 | 1.10 | - | - | - | **-** |
| 7 | 6.68 | 0.72 | 48 | 6.62 | 0.71 | **-0.9** |
| 8 | 6.81 | 0.54 | 50 | 6.92 | 0.81 | **1.6** |
| 9 | 7.13 | 0.34 | 49 | 6.62 | 0.92 | **-7.2** |
| 10 | 9.65 | 0.63 | 65 | 9.56 | 0.81 | **-0.9** |

**Wetteren footbridge**

| $\tilde{N}$ | $\tilde{f}$ [Hz] | $\tilde{\xi}$ [%] | N | $f$ [Hz] | MAC [−] | $\varepsilon$ [%] |
|---|---|---|---|---|---|---|
| 1 | 0.71 | 2.12 | 1 | 0.74 | 0.89 | **3.9** |
| 2 | 1.67 | 0.21 | 2 | 1.74 | 0.93 | **4.1** |
| 3 | 1.77 | 0.59 | - | - | - | **-** |
| 4 | 2.14 | 1.90 | - | - | - | **-** |
| 5 | 2.19 | 0.55 | 3 | 2.36 | 0.99 | **7.9** |
| 6 | 3.74 | 0.76 | 4 | 3.25 | 0.86 | **-13.2** |
| 7 | 3.84 | 0.67 | 5 | 3.83 | 0.90 | **-0.1** |
| 8 | 3.95 | 0.59 | - | - | - | **-** |
| 9 | 4.44 | 0.56 | 8 | 3.89 | 0.89 | **-12.4** |
| 10 | 5.14 | 1.15 | 9 | 3.94 | 0.82 | **-23.4** |

**Knokke footbridge**

| $\tilde{N}$ | $\tilde{f}$ [Hz] | $\tilde{\xi}$ [%] | N | $f$ [Hz] | MAC [−] | $\varepsilon$ [%] |
|---|---|---|---|---|---|---|
| 1 | 1.55 | 0.14 | 9 | 1.67 | 0.97 | **7.7** |
| 2 | 2.04 | 0.54 | 14 | 2.39 | 0.93 | **17.2** |
| 3 | 2.35 | 0.26 | 11 | 2.25 | 0.92 | **-4.3** |
| 4 | 2.58 | 0.64 | 20 | 2.95 | 0.94 | **14.3** |
| 5 | 2.74 | 1.24 | 20 | 2.95 | 0.76 | **7.7** |
| 6 | 2.97 | 0.81 | 23 | 3.22 | 0.95 | **8.4** |
| 7 | 3.34 | 0.36 | 17 | 2.58 | 0.70 | **-22.8** |
| 8 | 3.83 | 0.57 | 39 | 4.99 | 0.84 | **30.3** |
| 9 | 4.03 | 0.74 | 33 | 4.42 | 0.68 | **9.7** |
| 10 | 4.35 | 0.32 | 35 | 4.61 | 0.65 | **6.0** |

**Ninove footbridge**

| $\tilde{N}$ | $\tilde{f}$ [Hz] | $\tilde{\xi}$ [%] | N | $f$ [Hz] | MAC [−] | $\varepsilon$ [%] |
|---|---|---|---|---|---|---|
| 1 | 2.97 | 1.18 | 1 | 2.93 | 0.98 | **-1.5** |
| 2 | 3.06 | 1.92 | 2 | 2.06 | 0.69 | **-32.8** |
| 3 | 3.79 | 0.78 | - | - | - | **-** |
| 4 | 6.00 | 0.68 | 4 | 5.69 | 0.91 | **-5.2** |
| 5 | 6.93 | 0.59 | 6 | 7.24 | 0.94 | **4.5** |
| 6 | 7.99 | 0.78 | 7 | 7.69 | 0.82 | **-3.8** |
| 7 | 9.73 | 1.12 | 10 | 10.89 | 0.72 | **11.9** |

**Leuven footbridge**

| $\tilde{N}$ | $\tilde{f}$ [Hz] | $\tilde{\xi}$ [%] | N | $f$ [Hz] | MAC [−] | $\varepsilon$ [%] |
|---|---|---|---|---|---|---|
| 1 | 3.06 | 2.47 | 1 | 2.92 | 0.98 | **-4.6** |
| 2 | 4.82 | 5.93 | 2 | 4.37 | 0.90 | **-9.3** |
| 3 | 5.51 | 2.48 | 3 | 4.98 | 0.97 | **-9.6** |
| 4 | 6.61 | 2.89 | - | - | - | **-** |
| 5 | 7.92 | 2.19 | 4 | 5.93 | 0.78 | **-25.1** |
| 6 | 8.98 | 5.10 | - | - | - | **-** |

**Mechelen footbridge**

| $\tilde{N}$ | $\tilde{f}$ [Hz] | $\tilde{\xi}$ [%] | N | $f$ [Hz] | MAC [−] | $\varepsilon$ [%] |
|---|---|---|---|---|---|---|
| 1 | 3.75 | 1.08 | 2 | 3.70 | 0.99 | **-1.3** |
| 2 | 4.39 | 3.70 | - | - | - | **-** |
| 3 | 7.60 | 4.00 | 3 | 7.14 | 0.80 | **-6.1** |

**Brugge footbridge**

| $\tilde{N}$ | $\tilde{f}$ [Hz] | $\tilde{\xi}$ [%] | N | $f$ [Hz] | MAC [−] | $\varepsilon$ [%] |
|---|---|---|---|---|---|---|
| 1 | 1.64 | 0.24 | 1 | 1.86 | | **13.4** |
| 2 | 3.69 | 0.18 | 2 | 5.1 | | **38.2** |
| 3 | 6.55 | 0.16 | 3 | 8.86 | | **35.3** |

Table 6: Identified modal characteristics (mode number $\tilde{N}$, natural frequency $\tilde{f}$, damping ratios $\tilde{\xi}$) for all modes with a frequency up to 10 Hz and corresponding predicted natural frequencies of the numerical model ($f$), the Modal Assurance Criterion (MAC) and the relative frequency deviation ($\varepsilon$), for all case studies (the number of modes is limited to 10 for reasons of conciseness).

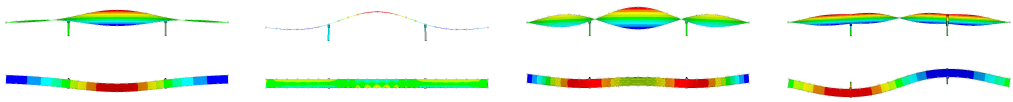

Figure 4: Vertical (top) and lateral (bottom) modal displacements of mode 1 up to 4 (left to right) of the Eeklo Footbridge

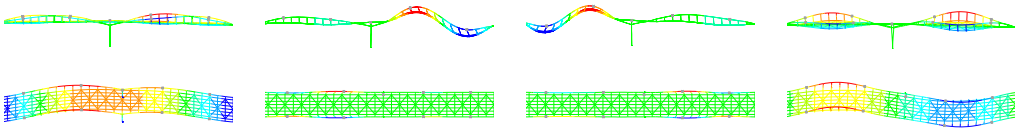

Figure 5: Vertical (top) and lateral (bottom) modal displacements of mode 1 up to 4 (left to right) of the Anderlecht Footbridge

shapes of the developed finite element model and the damping ratio as suggested by the guidelines. The vibration serviceability assessment requires the prediction of the maximum acceleration levels in each vibration direction. For all modes with a natural frequency less then 5 Hz, the predicted vertical maximum accelerations and corresponding comfort levels are summarised in figure 8 and 10 for the Eeklo and Anderlecht footbridge respectively. The corresponding mode shapes are presented in figures 4 and 5. As far as the assessment of the lateral vibrations is concerned, only the first mode of the Eeklo footbridge has a significant lateral component and a natural frequency in the corresponding range of interest (figure 9). The longitudinal vibrations were found to be negligible for these case studies.

In each figure, the maximum acceleration level predicted according to the Sétra and the HiVoSS guideline is presented for the different pedestrian densities and the corresponding comfort level is identified.

Apart from the single value for the maximum expected structural response based on the natural frequencies and mode shapes of the FE model, these figures present the range of predicted acceleration levels when the actual natural frequency is assumed to be situated within a range of $\pm 10\%$ of the predicted value. A number of interesting observations can be made.

*Predicted natural frequencies*

As a result of the strong variations of the reduction factor (figure 1), the predictions are highly sensitive to small variations in natural frequency of the considered mode. This is illustrated in figures 8 and 10 by the large range

in maximum acceleration levels resulting from the considered uncertainty of 10% on the predicted natural frequencies. When the natural frequencies all remain situated in the range corresponding to a high probability of resonance ($\psi_{eh} = 1$), the predicted maximum acceleration is much less sensitive to small variations in frequencies. This is the case for the third mode of Anderlecht (figure 10c).

In the analysis, the modification of the natural frequencies due to the mass of the pedestrians on the bridge deck has to be taken into account as well (see section 2.2). The added mass will result into a lower value for the predicted natural frequencies together with a decrease of the corresponding mass normalised modal displacements. Equation 5 shows that this decrease in modal displacements directly reduces the predicted acceleration levels. An interesting observation is that the change in natural frequency and modal displacements that results from an increase in pedestrian density, is different for each mode (table 7). For the first and the third mode of the Anderlecht footbridge, a change up to 20 % for the highest pedestrian density can be observed. The sensitivity of the mode to the added mass of the pedestrians depends on the magnitude of the modal deformations of the bridge deck.

The guidelines in their present form could be exploited by designers that tune the dynamic characteristics of the structure such that the footbridge passes the vibration serviceability check. Design parameters can be slightly adjusted to shift the predicted natural frequencies such that the reduction factor reaches a low value, e.g. in the narrow frequency range between the first and second harmonic (figure 1), leading to a lower predicted maximum structural response. Given the expected uncertainty on the predicted natural frequencies of the structure and considering in addition the influence of the added mass, it is suggested to apply the loading coefficient as presented in figure 6 when the assessment is performed in design stage. This loading coefficient is defined as the product of the dynamic load factor (table 2) and the original reduction factor (figure 1) for which the frequency bounds have been widened by 15% with respect to the center frequency of each interval. The corresponding predictions are presented in figures 8, 9 and 10 as well, and for the greater part correspond to the largest value obtained for the previously considered range of natural frequencies.

*Assumed damping ratios*

Damping ratios have an important influence on the predictions (see equation 5) but are difficult to estimate accurately in design stage. Generally,

**Eeklo footbridge**

| | Pedestrian density $d$ [p/m$^2$] | | | | | |
|---|---|---|---|---|---|---|
| | 15p | 0.2 | 0.5 | 0.8 | 1.0 | 1.5 |
| $f_1$ | 2.02 | 2.00 | 1.95 | 1.91 | 1.89 | 1.83 |
| $\Delta$ | -0.3 | -1.5 | -3.6 | -5.6 | -6.8 | -9.7 |
| $f_2$ | 3.07 | 3.02 | 2.92 | 2.83 | 2.78 | 2.65 |
| $\Delta$ | -0.5 | -2.3 | -5.5 | -8.4 | -10.2 | -14.2 |
| $f_3$ | 4.02 | 3.99 | 3.92 | 3.85 | 3.81 | 3.71 |
| $\Delta$ | -0.3 | -1.2 | -2.9 | -4.5 | -5.6 | -8.0 |
| $f_4$ | 4.78 | 4.73 | 4.63 | 4.53 | 4.47 | 4.33 |
| $\Delta$ | -0.3 | -1.5 | -3.6 | -5.5 | -6.8 | -9.7 |

**Anderlecht footbridge**

| | Pedestrian density $d$ [p/m$^2$] | | | | | |
|---|---|---|---|---|---|---|
| | 15p | 0.2 | 0.5 | 0.8 | 1.0 | 1.5 |
| $f_1$ | 3.08 | 2.94 | 2.83 | 2.71 | 2.64 | 2.49 |
| $\Delta$ | -0.7 | -5.4 | -8.8 | -12.7 | -14.9 | -19.9 |
| $f_2$ | 3.02 | 2.96 | 2.85 | 2.76 | 2.70 | 2.57 |
| $\Delta$ | -0.7 | -2.6 | -6.0 | -9.2 | -11.1 | -15.5 |
| $f_3$ | 3.75 | 3.66 | 3.49 | 3.34 | 3.25 | 3.05 |
| $\Delta$ | -1.0 | -3.4 | -8.0 | -12.0 | -14.4 | -19.5 |
| $f_4$ | 4.48 | 4.43 | 4.34 | 4.27 | 3.93 | 3.82 |
| $\Delta$ | -0.4 | -1.5 | -3.5 | -5.1 | -12.7 | -15.1 |

Table 7: Modification of the natural frequencies ($\Delta$ [%]) due to the added mass of the pedestrians on the bridge deck (70 kg/person) corresponding to the considered pedestrian density.

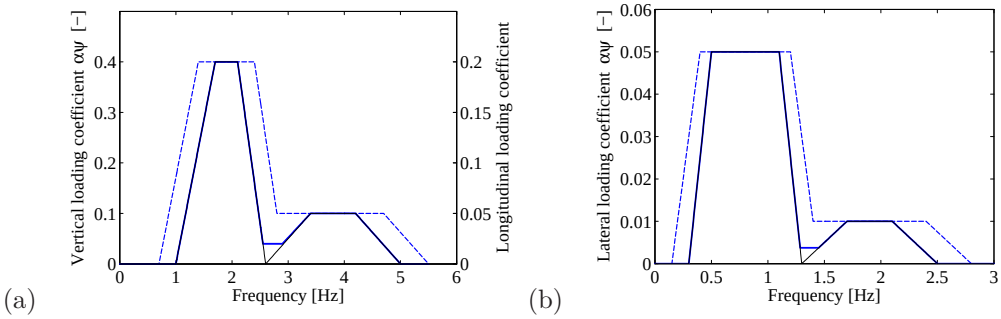


(a) (b)

Figure 6: Suggested loading coefficient $\alpha\psi(f_j)$ to apply respectively (- -) in design stage and (–) at completion, and (black) the corresponding original coefficient as defined by Sétra and HiVoSS (a) for vertical, longitudinal and, (b) lateral loading.

damping coefficients ranging between 0.1% and 2.0% are used. It is best not to overestimate structural damping in order to ensure a conservative prediction of the maximum acceleration levels. The guidelines suggest different damping ratios according to the construction type (table 3). In case of steel structures, a minimum value of 0.2% and mean value of 0.4% are suggested. The modal damping ratios identified from in situ tests for all bridges considered in this study (all steel structures) are presented in figure 7. These results generally seem to confirm the values recommended in the guidelines: only a limited number of modes have an identified modal damping ratio (slightly) below the proposed minimum of 0.2% and the mean value of 0.4% seems to be a reasonable assumption. It can also be observed that modal damping ratios of bending modes range between 0.15 and 0.9%, whereas for torsional

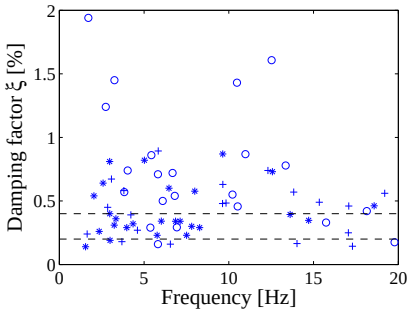


Figure 7: Identified modal damping ratios of the investigated footbridges as a function of the corresponding natural frequency, for (∗) vertical bending, (+) lateral bending and (∘) torsional modes. The upper and lower dashed line represent the mean and minimum damping value, respectively, as suggested by the guidelines for steel structures.

modes damping ratios may increase up to 2% or more. It has to be acknowledged that the in situ identified damping ratios are also subjected to some degree of uncertainty.

Considering a mean damping ratio of 0.4% in design stage and assessing the vibrational behaviour of the structure for different traffic classes will allow for the identification of modes that are critical for the vibration serviceability. In addition, the designer must keep in mind that the damping ratios may even have lower values. It is therefore recommended to verify the modal parameters once the footbridge is built.

*Dense or sparse crowd conditions*

Figures 8 and 10 also illustrate that once *dense* crowd conditions are considered, a rather abrupt increase in the predicted acceleration levels occurs. This is due to the way in which the number of equivalent pedestrians is calculated (section 2.1) in *dense* and *sparse* crowd conditions. This increase in vibration level is even more emphasised for the case of low damping ratios where the number of equivalent pedestrians is even lower in *sparse* crowd conditions (equation 3).

*Assessment of the lateral vibrations*

All natural frequencies with the exception of the first mode of the Eeklo footbridge, exceed the range of the second harmonic of the lateral walking load. Therefore, when predicting the lateral vibration levels, only resonant conditions have to be considered for that specific mode. The corresponding

assessment of the lateral vibrations is presented in figure 9. The HiVoSS guideline does not consider the second harmonic of the lateral load, so that these results are not included here (as noted in subsection 2.5).

Based on the results presented in figure 9, no problems of vibration serviceability are expected. It should be noted, however, that only the component of the walking force in the considered lateral vibration direction is taken into account. In case of bending modes with modal displacements that are significant in only the vertical or lateral direction, this is an assumption that is justified. For modes with significant modal displacements in more then one direction, however, the vibration levels could be significantly underestimated. This can be the case in particular for the predicted lateral response since the amplitude of the vertical component of the walking load is significantly larger (table 2), i.e. even relatively small vertical modal displacements may give rise to considerable lateral vibrations. Further examination is required to investigate the implications so that it can be addressed adequately.

*Expected vibration comfort*

In this section, the vibration serviceability is assessed in design stage for the Eeklo and Anderlecht footbridge, following the above formulated recommendations to account for uncertainty on the predicted natural frequencies.

The evaluation of the first mode (figures 8a and 9) and second mode (figure 8b) of the Eeklo footbridge, indicate potentially lively behaviour with unacceptable vibration levels in case of dense traffic conditions. No problems are expected for the fourth mode (figure 8d) and maximum comfort is ensured for the third mode in case of low pedestrian densities (figure 8c). The second mode is in this case clearly the critical mode in the global assessment. The predicted acceleration levels are, however, extremely high and will most probably not occur due to (1) the expected increase in damping for larger vibration amplitudes and (2) the self-limiting nature of the pedestrian induced loading [32, 33, 34].

This assessment does indicate the high sensitivity of this mode to human induced vibrations. Vibration comfort cannot be assured for pedestrian densities of 0.5 p/m$^2$ or more. Given the limited occupation expected for the rural environment of the Eeklo footbridge, this is not considered a problem. For the occasional passage of larger groups of pedestrians, however, vibration comfort is not assured.

Figure 10a shows that excitation of the first mode of the Anderlecht footbridge will not lead to high vertical vibration levels, which is due to the dis-

tinct lateral movement of the mode (figure 5). Maximum comfort is ensured for the fourth mode, a torsional mode with a significant lateral component, for all pedestrian densities. Evaluation of mode two and three indicates potentially lively behaviour with minimum comfort for low pedestrian densities and unacceptable vibration levels for dense traffic conditions. The very high predicted vibration levels for both modes result from large modal displacements and thus low modal mass, indicating the distinctly lively behaviour of the structure. This assessment made at design stage suggests that a modification of the structural design or the implementation of vibration mitigation measures is required.

*4.2. At completion*

Once the footbridge is constructed, the modal parameters of the structure can be identified in situ. A more reliable prediction of the expected vibration comfort of the pedestrians can now be obtained by using the experimentally identified natural frequencies and damping ratios.

Figure 6 presents the loading coefficient suggested in the case where the modal characteristics have been identified from in situ vibration measurements. The suggested loading coefficient is similar to the one defined by the guidelines but differs in between the intervals of the first and second harmonic where it is suggested to maintain a certain minimum level. This will allow identifying modes that are highly sensitive to human induced vibrations, with a natural frequency within that specific range. An additional argument to maintain that minimum level in between the first and second harmonic of the loading frequency, is the fact that also sub- and intermediate harmonics are being observed [22]. These intermediate harmonics are the result of small differences between left and right foot and are usually disregarded because they have relatively low amplitudes.

When a good agreement between the relevant predicted and identified modes is found ($f_j < 5$Hz), the vibration serviceability can be assessed based on the in situ identified natural frequencies, modal damping ratios, and corresponding predicted mode shapes. However, when relevant modes identified from in situ tests are not predicted by the numerical model, e.g. for the Mechelen, Ninove and Wetteren footbridge (table 6), it is recommended to revise the finite element model. A possible solution can be to tune or calibrate the FE model in order to obtain a better the agreement between the calculated and identified natural frequencies and mode shapes [9, 35].

For both the Eeklo and the Anderlecht footbridge, all relevant modes were identified by the initial finite element model. The results of the reassessment of the vibration serviceability based on the in situ identified natural frequencies and modal damping ratios, are presented in figures 11 up to 13. The error bars present the range of predicted acceleration levels when considering the influence of the additional mass on the natural frequencies and mode shapes of the FE model. The range of the predicted acceleration levels is significantly smaller than in design stage, since the uncertainty with respect to the natural frequencies can now be excluded. In view of a safe design, it is recommended to perform the vibration serviceability assessment based on the maximum value. By way of comparison, the results of the initial assessment in design stage are shown as well.

*Eeklo footbridge*

From the assessment in design stage, it was found that the first three modes as potentially critical modes in case of high pedestrian densities. Due to the high values of the identified modal damping ratios, a maximum level of comfort is still ensured for all pedestrian densities for the first and the third mode. The second mode, however, has a low modal damping ratio ($\xi = 0.2\%$), and in this case a minimum level of comfort is expected for sparse pedestrian densities. Given the distinct rural environment of this footbridge with limited occupation ($\leq 0.2$ p/m$^2$), maximum up to mean comfort is expected which results into a satisfactory vibration performance of this footbridge. In case of increased pedestrian traffic, it is clear that the vibration comfort of the pedestrians is at risk for pedestrian densities higher then 0.2 p/m$^2$. This assessment has, however, identified the critical mode and provides the necessary insights to take the proper vibration mitigation measures.

*Anderlecht footbridge*

Taking into account the measured frequencies and modal damping ratios does not modify the results of the vibration serviceability assessment that was made before for the Anderlecht footbridge. Potentially lively behaviour was identified for modes two and three, leading to minimum comfort up to unacceptable vibration levels for respectively sparse and dense pedestrian densities. Despite of the rather rural environment of the Anderlecht footbridge, this assessment suggests a modification of the structural design or

the application of adequate vibration countermeasures. The assessment performed at completion has again identified the critical modes and enables a focused intervention.

*Overview of the investigated footbridges*

In this final section, the results of the vibration serviceability assessment are summarised for all cases. The predicted maximum response for the critical mode and corresponding expected comfort level are presented in figures 14 and 15, for the vertical and lateral vibrations, respectively. These results show that adapting the loading coefficient as suggested, allows accounting for the uncertainties of the dynamic properties of the structure in design stage.

The lateral vibration serviceability check was only required for a limited number of the investigated footbridges as a result of the low upper bound of the frequency range of interest for the lateral vibrations. Figure 15 shows that the predicted response in these cases remains acceptable. For the Knokke and the Eeklo footbridge, however, the lateral response could be underestimated due to the distinct torsional behaviour of the considered mode which makes them also sensitive to vertical loading (section 4.1).

Figure 14a shows that for the *sparse* pedestrian density of 0.8 p/m$^2$, minimum comfort or unacceptable vibration levels are predicted in four cases. Only one of these cases, the Mechelen footbridge, is located in a city center where urban use and high pedestrian densities are expected. These potentially disturbing vibration levels were already identified in design stage and therefore it was decided to include a tuned mass damper (TMD). In a previous study, an equivalent modal damping ratio was derived to account for the effect of the TMD, showing that the applied vibration mitigation measure ensures the vibration comfort even for high pedestrian densities [9].

In figure 14b, the predicted response is presented for *dense* traffic conditions. The Eeklo, Knokke and Anderlecht footbridge stand out with very high acceleration levels, indicating a strong sensitivity to human induced vibrations. For these cases, one should be particularly conscious of the comfort requirements. Additionally, future changes in pedestrian traffic have to be considered, e.g. due to reallocation in spatial planning and development [18].

## 5. Conclusions

Pedestrian bridges are very often lively structures prone to human induced vibrations, necessitating the vibration serviceability assessment in de-

sign stage. The current codes of practice (Sétra and HiVoSS) enable the designer to check the vibration serviceability of the footbridge based on a prediction of the maximum acceleration levels. The guides present a selection of pedestrian densities and apply a simplified equivalent load model to represent crowd induced loading.

The methodology of these codes of practice is discussed and reviewed with respect to their application in design stage and at completion. In total, eight steel footbridges have been studied. For each case, a finite element model was developed to simulate the physical behaviour of the structure and to predict the response under human induced loading.

In design stage, uncertainty with regard to the predicted dynamic properties of the footbridge is inevitable. It is shown that even with the development of a detailed finite element model, deviations up to 10% in terms of natural frequencies can be expected. The evaluations made by the codes of practice are found to be highly sensitive to small variations in predicted natural frequencies. The authors have therefore suggested a modified load model that accounts for uncertainty in predicted natural frequencies in design stage.

Damping properties have an important influence on the predictions but are difficult to estimate in design phase. The identified damping properties of the investigated footbridges, confirm the recommended values of the guidelines.

Once the footbridge is built, an in situ identification of modal parameters is recommended. The identified modal characteristics can be applied to reassess the vibration serviceability, in order to get a more reliable prediction of the expected vibration comfort of the pedestrians. If necessary, the proper vibration countermeasures should be taken.

## 6. Acknowledgements

The results of this paper were partly obtained within the framework of the research project, TRICON "Prediction and control of human-induced vibrations of civil engineering structures", financed by the Flemish government (IWT, agency for Innovation by Science and Technology).

The authors would like to thank the engineering offices and parties concerned for their cooperation and providing information on the investigated footbridges.

## References


[1] S. Živanović, A. Pavic, and P. Reynolds, "Vibration serviceability of footbridges under human-induced excitation: a literature review," *Journal of Sound and Vibration*, vol. 279, no. 1-2, pp. 1–74, 2005.

[2] P. Dallard, T. Fitzpatrick, A. Flint, S. Bourva, A. Low, and e. a. Ridsdill Smith, R.M., "The London Millennium footbridge," *The Structural Engineer*, no. 79, pp. 17–33, 2001.

[3] P. Dallard, T. Fitzpatrick, A. Flint, A. Low, R. Smith, M. Willford, and M. Roche, "The London Millennium footbridge: Pedestrian-Induced Lateral Vibration," *Journal of Bridge Engineering*, vol. 6, pp. 412–417, 2001.

[4] P. Dziuba, G. Grillaud, O. Flamand, S. Sanquier, and Y. Tétard, "La passerelle Solférino comportement dynamique (dynamic behaviour of the Solférino bridge)," *Bulletin Ouvrages Métalliques*, vol. 1, pp. 34–57, 2001.

[5] E. Caetano, A. Cunha, F. Magalhães, and C. Moutinho, "Studies for controlling human-induced vibration of the Pedro e Inês footbridge, Portugal. Part 1: Assessment of dynamic behaviour," *Engineering Structures*, vol. 32, pp. 1069–1081, 2010.

[6] E. Caetano, A. Cunha, F. Magalhães, and C. Moutinho, "Studies for controlling human-induced vibration of the Pedro e Inês footbridge, Portugal. Part 2: Implementation of tuned mass dampers," *Engineering Structures*, vol. 32, pp. 1082–1091, 2010.

[7] J. Brownjohn, P. Fok, M. Roche, and P. Moyo, "Long span steel pedestrian bridge at Singapore Changi Airport - part 1: Prediction of vibration serviceability problems," *The Structural Engineer*, vol. 82, no. 16, pp. 21–27, 2004.

[8] J. Brownjohn, P. Fok, M. Roche, and P. Omenzetter, "Long span steel pedestrian bridge at Singapore Changi Airport - part 2: Crowd loading tests and vibration mitigation measures," *The Structural Engineer*, vol. 82, no. 16, pp. 28–34, 2004.

[9] K. Van Nimmen, P. Van den Broeck, B. Gezels, G. Lombaert, and G. De Roeck, "Experimental Validation of the Vibration Serviceability Assessment of a Lightweight Steel Footbridge with Tuned Mass Damper," in *Proceedings of the 25th Conference on Noise and Vibration Engineering*, (Leuven, Belgium), September 2012.

[10] C. Butz, C. Schuermann, and O. Benicke, "Tuned mass dampers for the footbridge of VW Autostadt in Wolfsburg, Germany," in *Proceedings of the 4th International Footbridge Conference*, (Wroclaw, Poland), July 2011.

[11] I. Ainsworth, K. Franklin, and P. Burnton, "Kurilpa brigde - a case study," in *Proceedings of the 4th International Footbridge Conference*, (Wroclaw, Poland), July 2011.

[12] C. Meinhardt, "Detailed numerical and experimental dynamic analysis of long-span footbridges to optimize structural control measures," in *Proceedings of the 6th International Conference on Bridge Maintenance, Safety and Management*, (Stresa, Italy), July 2012.

[13] G. Piccardo and F. Tubino, "Equivalent spectral model and maximum dynamic response for the serviceability analysis of footbridges," *Engineering Structures*, vol. 40, pp. 445–456, 2012.

[14] W. Dong, M. Kasperski, and G. Shiqiao, "Change of the dynamic characteristics of a pedestrian bridge during a mass event," in *Proceedings of the 8th International Conference on Structural Dynamics of EURODYN*, (Leuven, Belgium), July 2011.

[15] Q. Li, J. Fan, J. Nie, Q. Li, and Y. Chen, "Crowd-induced random vibration of footbridge and vibration control using multiple tuned mass dampers," *Journal of Sound and Vibration*, no. 329, pp. 4068–4092, 2010.

[16] F. Venuti and L. Bruno, "Crowd-structure interaction in lively footbridges under synchronous lateral excitation: a literature review," *Physics of Life Reviews*, vol. 6, pp. 176–206, 2009.

[17] V. Racic, A. Pavic, and P. Reynolds, "Experimental identification and analytical modelling of walking forces: a literature review," *Journal of Sound and Vibration*, vol. 326, pp. 1–49, 2009.

[18] Association Franaise de Génie Civil, Sétra/AFGC, *Sétra: Evaluation du comportement vibratoire des passerelles piétonnes sous l'action des piétons*, 2006.

[19] Research Fund for Coal and Steel, *HiVoSS: Design of footbridges*, 2008.

[20] C. Butz, M. Feldmann, C. Heinemeyer, and G. Sedlacek, "SYNPEX: Advanced load models for synchronous pedestrian excitation and optimised design guidelines for steel footbridges," report, Research Fund for Coal and Steel, 2007.

[21] C. Caprani, J. Keogh, P. Archbold, and P. Fanning, "Enhancement for the vertical response of footbridges subjected to stochastic crowd loading," *Computers and Structures*, vol. 102-103, pp. 87–96, 2012.

[22] C. Sahnaci and M. Kasperski, "Simulation of random pedestrian flow," in *Proceedings of the 8th International Conference on Structural Dynamics of EURODYN*, (Leuven, Belgium), July 2011.

[23] M. Bocian, J. Macdonald, and J. Burn, "Biomechanically inspired modelling of pedestrian-induced forces on laterally oscillating structures," *Journal of Sound and Vibration*, vol. 331, pp. 3914–3929, 2012.

[24] S. Carroll, J. Owen, and M. Hussein, "Modelling crowd-bridge dynamic interaction with a discrete defined crowd," *Journal of Sound and Vibration*, vol. 331, no. 11, pp. 2685–2709, 2012.

[25] Y. Matsumoto, S. Maeda, Y. Iwane, and Y. Iwata, "Factors affecting perception thresholds of vertical whole-body vibration in recumbent subjects: gender and age of subjects and vibration duration," *Journal of Sound and Vibration*, vol. 330, no. 8, pp. 1810–1828, 2011.

[26] Y. Matsumoto, T. Nishioka, H. Shiojiri, and K. Matsuzaki, "Dynamic design of footbridges," in *IABSE Proceedings*, P-17/78, pp. 1–15, 1978.

[27] G. Tilly, D. Cullington, and R. Eyre, "Dynamic behaviour of footbridges," *IABSE Periodical*, vol. S-26/84, 1984.

[28] J. Wheeler, "Prediction and control of pedestrian-induced vibrations in footbridges," *ASCE Journal of Structural Engineering*, vol. 108, no. ST9, 1982.

[29] B. Peeters and G. De Roeck, "Reference-based stochastic subspace identification for output-only modal analysis," *Mechanical Systems and Signal Processing*, vol. 13, no. 6, pp. 855–878, 1999.

[30] E. Reynders and G. De Roeck, "Reference-based combined deterministic-stochastic subspace identification for experimental and operational modal analysis," *Mechanical Systems and Signal Processing*, vol. 22, no. 3, pp. 617–637, 2008.

[31] E. Reynders, R. Pintelon, and G. De Roeck, "Uncertainty bounds on modal parameters obtained from Stochastic Subspace Identification," *Mechanical Systems and Signal Processing*, vol. 22, no. 4, pp. 948–969, 2008.

[32] E. Ingolfson, *Pedestrian-induced lateral vibrations of footbridges: experimental studies and probabilistic modelling*. PhD thesis.

[33] S. Nakamura, "Model for lateral excitation of footbridges by synchronous walking," *ASCE Journal of Structural Engineering*, vol. 130, no. 1, pp. 32–37, 2011.

[34] J. Scheller and U. Starossek, "Design and experimental verification of a new active mass damper for control of pedestrian-induced bridge vibrations," in *Proceedings of the 4th International Footbridge Conference*, (Wroclaw, Poland), July 2011.

[35] E. Lourens, C. Papadimitriou, S. Gillijns, E. Reynders, G. De Roeck, and G. Lombaert, "Joint input-response estimation for structural systems based on reduced-order models and vibration data from a limited number of sensors," *Mechanical Systems and Signal Processing*, vol. 29, pp. 310–327, 2012.

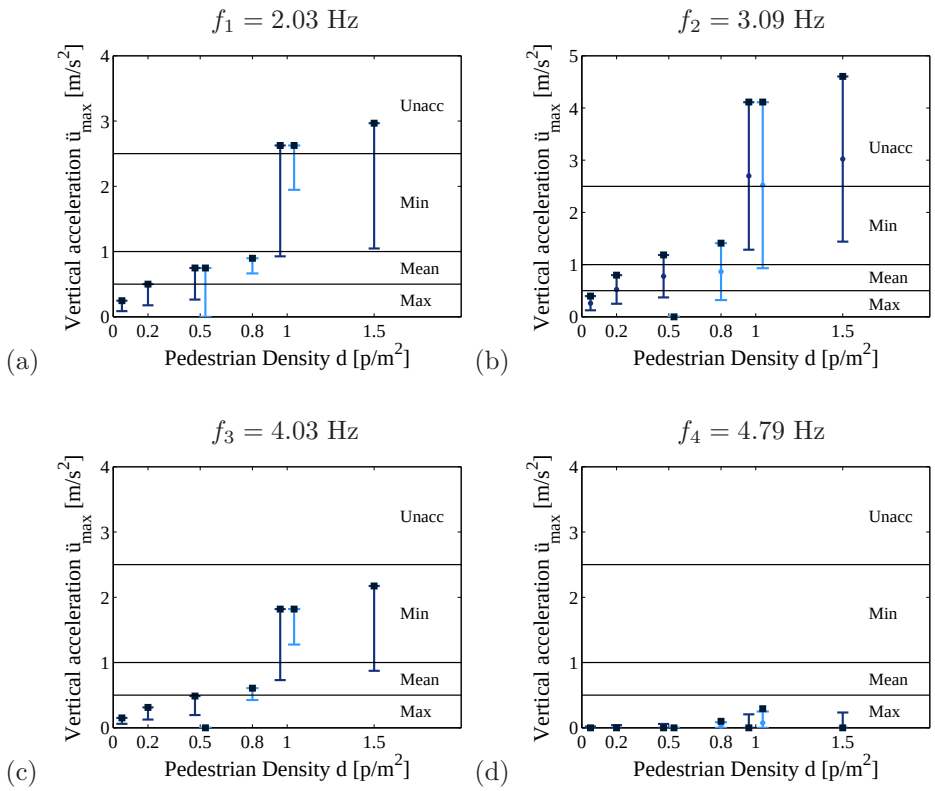


Figure 8: Predicted maximum vertical acceleration levels for the Eeklo footbridge in design stage according to Sétra (light) and HiVoSS (dark) for mode 1 (a), 2 (b), 3 (c) and 4 (d), considering a range of ±10% on the predicted natural frequencies (error bar). The black square represents the predicted maximum acceleration level corresponding to the loading coefficient recommended for the design stage.

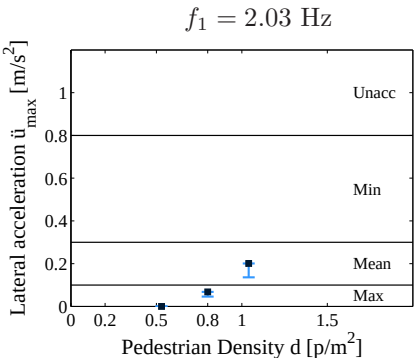


Figure 9: Predicted maximum lateral acceleration levels for the Eeklo footbridge in design stage according to Sétra (light) and HiVoSS (dark) for mode 1, considering a range of $\pm 10\%$ on the predicted natural frequencies (error bar). The black square represents the predicted maximum acceleration level corresponding to the loading coefficient recommended for the design stage.

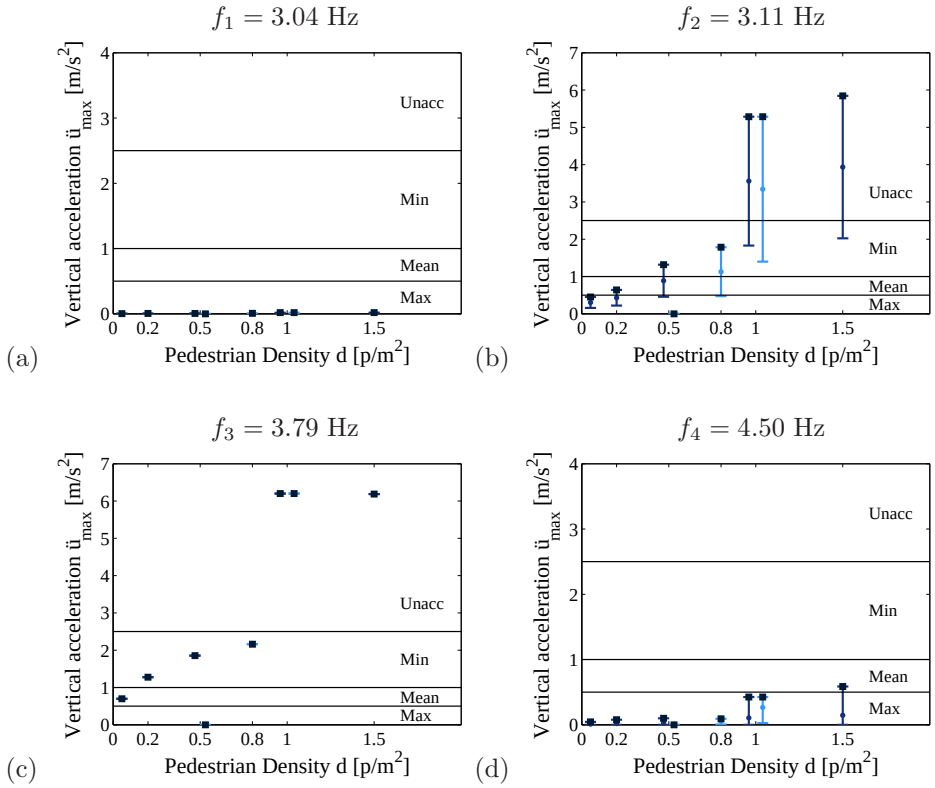


Figure 10: Predicted maximum vertical acceleration levels for the Anderlecht footbridge in design stage according to Sétra (light) and HiVoSS (dark) for mode 1 (a), 2 (b), 3 (c) and 4 (d), considering a range of ±10% on the predicted natural frequencies (error bar). The black square represents the predicted maximum acceleration level corresponding to the loading coefficient recommended for the design stage.

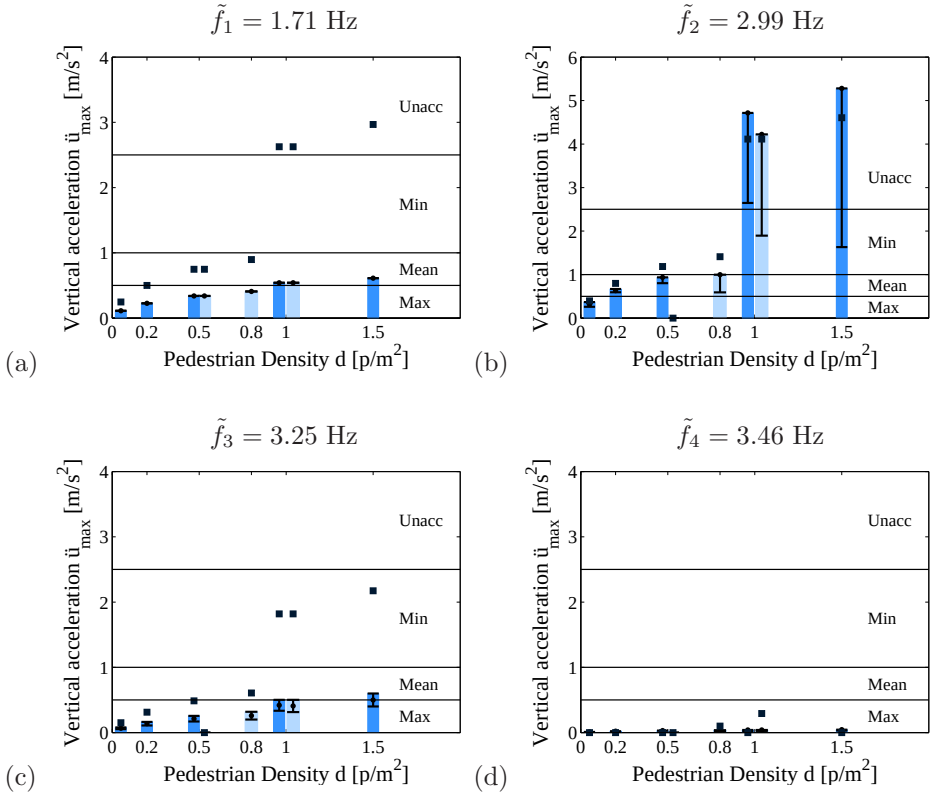


Figure 11: Upper bound of the predicted maximum vertical acceleration levels for the Eeklo footbridge at completion according to Sétra (light) and HiVoSS (dark) for mode 1 (a), 2 (b), 3 (c) and 4 (d) and the influence of the added mass of the considered pedestrian density (error bar). The black square represents the predicted maximum acceleration level in design stage corresponding to the recommended loading coefficient.

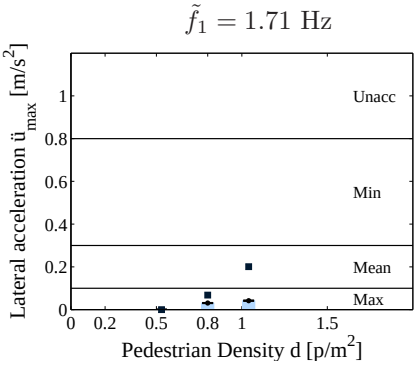


Figure 12: Upper bound of the predicted maximum lateral acceleration levels for the Eeklo footbridge at completion according to Sétra (light) and HiVoSS (dark) for mode 1 (a), 2 (b), 3 (c) and 4 (d) and the influence of the added mass of the considered pedestrian density (error bar). The black square represents the predicted maximum acceleration level in design stage corresponding to the recommended loading coefficient.

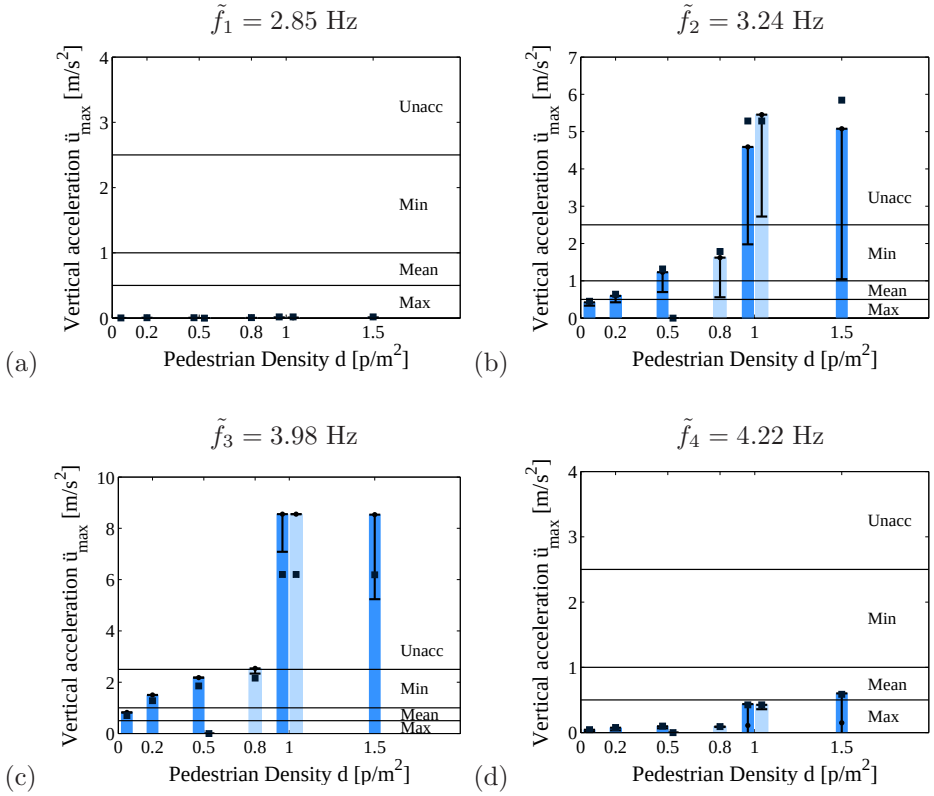


Figure 13: Upper bound of the predicted maximum vertical acceleration levels for the Anderlecht footbridge at completion according to Sétra (light) and HiVoSS (dark) for mode 1 (a), 2 (b), 3 (c) and 4 (d) and the influence of the added mass of the considered pedestrian density (error bar). The black square represents the predicted maximum acceleration level in design stage corresponding to the recommended loading coefficient.

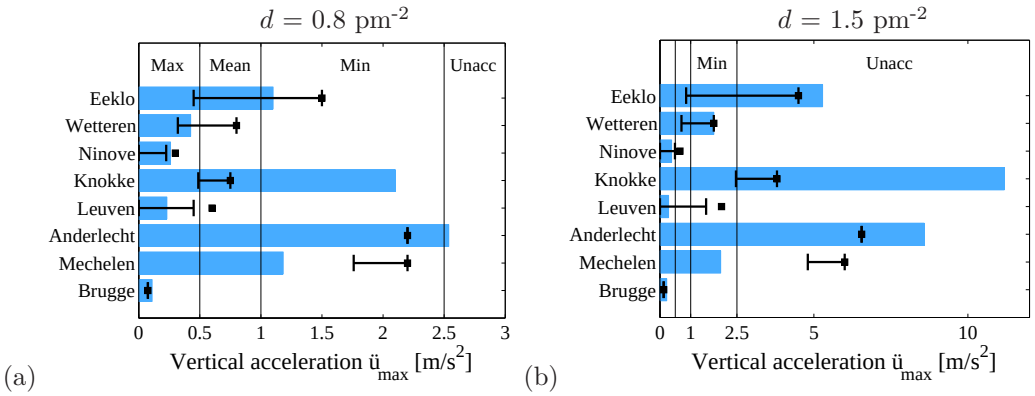


Figure 14: Predicted maximum vertical acceleration levels and corresponding comfort evaluation for the investigated footbridges at completion (color bar) and in design stage considering a range of ±10% on the predicted natural frequencies according to the guidelines (error bar) and considering the recommended loading coefficient (black square).

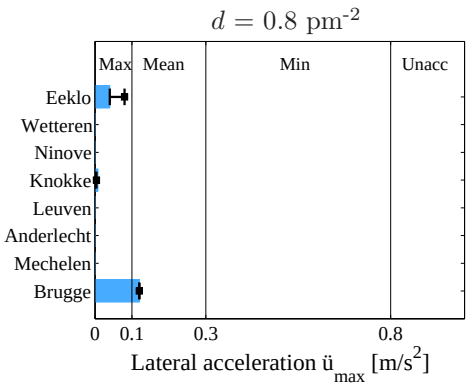


Figure 15: Predicted maximum lateral acceleration levels and corresponding comfort evaluation for the investigated footbridges at completion (color bar) and in design stage considering a range of ±10% on the predicted natural frequencies according to the guidelines (error bar) and considering the recommended loading coefficient (black square).